Disease Models & Mechanisms 6, 383-396 (2013) doi:10.1242/dmm.010249

TNF receptors regulate vascular homeostasis in zebrafish through a caspase-8, caspase-2 and P53 apoptotic program that bypasses caspase-3

Raquel Espín[1,2,*], Francisco J. Roca[1,3,*], Sergio Candel[1,2], María P. Sepulcre[1,2], Juan M. González-Rosa[4], Francisca Alcaraz-Pérez[1,2,5], José Meseguer[1,2], María L. Cayuela[2,5], Nadia Mercader[4] and Victoriano Mulero[1,2,‡]

SUMMARY

Although it is known that tumor necrosis factor receptor (TNFR) signaling plays a crucial role in vascular integrity and homeostasis, the contribution of each receptor to these processes and the signaling pathway involved are still largely unknown. Here, we show that targeted gene knockdown of TNFRSF1B in zebrafish embryos results in the induction of a caspase-8, caspase-2 and P53-dependent apoptotic program in endothelial cells that bypasses caspase-3. Furthermore, the simultaneous depletion of TNFRSF1A or the activation of NF-κB rescue endothelial cell apoptosis, indicating that a signaling balance between both TNFRs is required for endothelial cell integrity. In endothelial cells, TNFRSF1A signals apoptosis through caspase-8, whereas TNFRSF1B signals survival via NF-κB. Similarly, TNFα promotes the apoptosis of human endothelial cells through TNFRSF1A and triggers caspase-2 and P53 activation. We have identified an evolutionarily conserved apoptotic pathway involved in vascular homeostasis that provides new therapeutic targets for the control of inflammation- and tumor-driven angiogenesis.

INTRODUCTION

Tumor necrosis factor-α (TNFα) is a powerful pro-inflammatory cytokine produced and released mainly by mononuclear phagocytes that regulates endothelial cell functions and strongly and specifically alters their gene expression profile (Miura et al., 2006). TNFα exerts its functions through interaction with two specific cell surface receptors: the 55 kDa tumor necrosis factor receptor superfamily member 1A (TNFRSF1A) and the 75 kDa TNFRSF1B (Shalaby et al., 1990). TNFRSF1A is expressed in most cell types, even in transformed cells, whereas TNFRSF1B function seems to be restricted to immune and endothelial cells (Aggarwal, 2003). Recent studies with deficient mice have shown that TNFRSF1A predominantly triggers apoptosis or inflammation, whereas TNFRSF1B promotes tissue repair and regeneration (Aggarwal, 2003). Neither TNFRSF1A nor TNFRSF1B has intrinsic enzymatic activity, so they both need to recruit accessory proteins for signal transduction. Three main types of proteins interact with the cytoplasmic domains of TNFRs: TNFR-associated factors (TRAFs), FAS-associated via death domains (FADDs) and TNFR-associated via death domains (TRADDs). TNFRSF1A promotes the recruitment of TRAF2 and TRADD, which interact with several signaling proteins, such as the E3-ubiquitin ligases BIRC2 (cIAP1) and BIRC3 (cIAP2), to form complex I. This complex induces the proteasome-dependent degradation of the nuclear factor-κB (NF-κB) inhibitor IκB and, hence, nuclear translocation of NF-κB and the transcription of pro-inflammatory and survival genes (Locksley et al., 2001; MacEwan, 2002). A complex II can also be generated from complex I upon release from TNFRSF1A and recruitment of FADD and caspase-8, resulting in caspase-8 activation and leading to cell death (Locksley et al., 2001; MacEwan, 2002). By contrast, TNFRSF1B triggers the recruitment of TRAF1 and TRAF2, which interact with BIRC2 and BIRC3 (Rothe et al., 1995), leading to NF-κB activation.

Therefore, TNFα has been dubbed a 'double-edged sword' because it might initiate distinct or overlapping signal transduction pathways by binding to TNFRSF1A and/or TNFRSF1B, resulting in a variety of cellular responses, such as survival, differentiation, proliferation and migration, or, on the other hand, cell death (Aggarwal, 2003). This pleiotropic activity links TNFα with a wide variety of human diseases, including inflammatory and autoimmune disorders, ischemia-reperfusion injury and cancer.

Using a forward genetic approach in the zebrafish (*Danio rerio*), Santoro and co-workers identified BIRC2 as an essential molecule involved in maintaining endothelial cell survival and vascular homeostasis (Santoro et al., 2007). In the absence of BIRC2, a caspase-8- and caspase-3-dependent apoptotic program leads to vessel regression. Given that human BIRC2 plays a key role in the TNFRSF1B signaling pathway (Rothe et al., 1995) and that endothelial cells have been reported to be a major target for TNFα in fish (Roca et al., 2008), we used gain- and loss-of-function studies to analyze the role played by each TNFR in the development and maintenance of endothelial cells in this species. We found that

[1]Departmento de Biología Celular e Histología, Facultad de Biología, Universidad de Murcia, 30100 Murcia, Spain
[2]Instituto Murciano de Investigación Biosanitaria (IMIB), 30100 Murcia, Spain
[3]Department of Microbiology, University of Washington, Seattle, WA 98195, USA
[4]Departamento de Biología del Desarrollo Cardiovascular, Centro Nacional de Investigaciones Cardiovasculares, Melchor Fernández Almagro 3, 28029 Madrid, Spain
[5]Telomerase, Cancer and Aging Group, Research Unit, Department of Surgery, University Hospital 'Virgen de la Arrixaca', 30120 Murcia, Spain
*These authors contributed equally to this work.
‡Author for correspondence (vmulero@um.es)

Received 25 May 2012; Accepted 18 August 2012

TRANSLATIONAL IMPACT

Clinical issue

Tumor necrosis factor-α (TNFα) is a powerful pro-inflammatory cytokine that plays a prominent pathogenic role in many human diseases, including inflammatory and autoimmune disorders, ischemia-reperfusion injury and cancer. Although it is well known that TNFα signals through the receptors TNFRSF1A and TNFRSF1B, there are still outstanding questions about the signaling pathways associated with each receptor, and how each receptor contributes to the development of diseases is still largely unknown.

Results

This paper addresses this issue using the zebrafish embryo as a model system. The authors show that genetic depletion of TNFRSF1B in zebrafish embryos results in the induction of an apoptotic program in endothelial cells that requires caspase-8, caspase-2 and P53, but that bypasses caspase-3. Simultaneous depletion of TNFRSF1A, or activation of nuclear factor-κB (NF-κB), rescues endothelial cell apoptosis, indicating that a balance of signaling mediated by both receptors is required for endothelial cell integrity. Thus, TNFRSF1A triggers apoptosis via caspase-8, whereas TNFRSF1B promotes survival via NF-κB. Importantly, this apoptotic pathway seems to be evolutionarily conserved, as TNFα promotes apoptosis of human endothelial cells and triggers caspase-2 and P53 activation in these cells via TNFRSF1A.

Implications and future directions

Several systemic inhibitors of TNFα, such as soluble TNFα receptors and TNFα antibodies, have been approved for the treatment of human diseases in which TNFα plays a pathogenic role. However, these drugs have severe side effects and are expensive. Hence, new active blockers of TNFα that are safe, efficacious and inexpensive are urgently needed. The crucial balance of signaling between TNFRSF1A and TNFRSF1B identified in this study suggests that drugs specifically targeting TNFα receptors and their signaling adaptor molecules, rather than TNFα, could be developed to treat TNFα-driven human diseases.

targeted gene silencing of TNFRSF1B results in the induction of a caspase-8-dependent apoptotic program in endothelial cells that can be rescued by depletion of TNFRSF1A. This indicates that an appropriate signaling balance between both TNFRs is required for endothelial cell integrity and vascular homeostasis. In addition, the data also showed that, in endothelial cells, TNFRSF1A signals apoptosis through complex II formation and caspase-8 activation, whereas TNFRSF1B signals survival via complex I and NF-κB activation. Furthermore, we were able to establish a TNFRSF1A apoptotic program that involved caspase-8, caspase-2 and P53, but bypassed caspase-3. The molecular mechanism proposed applies not only for the zebrafish because activation of TNFRSF1A also promoted apoptosis and caspase-2 and P53 activation in human endothelial cells following TNFα treatment. This evolutionarily conserved apoptotic pathway involved in vascular development and homeostasis places TNFRs and caspase-2 in the front line for inflammatory, angiogenesis and tumor drug development.

RESULTS

Genetic depletion of TNFRSF1B results in blood circulation disruption, blood pooling and vascular hemorrhage

The zebrafish has single orthologs of mammalian TNFRSF1A and TNFRSF1B, which showed 38% amino acid similarity to their human counterparts and conserved TNFR superfamily and death domains (Grayfer and Belosevic, 2009). In addition, we confirmed by pull-down assay that TNFα was able to bind both TNFRs (supplementary material Fig. S1). Gene expression analysis by quantitative real-time reverse transcriptase polymerase chain reaction (RT-qPCR) showed that the mRNA of both TNFRs was present in zebrafish embryos at spawning, indicating that it was maternally transferred (supplementary material Fig. S2A). However, the expression profiles of genes encoding the two TNRFs were different: whereas the mRNA levels for TNFRSF1A drastically increased 24 hours post-fertilization (hpf) and reached a plateau, those for TNFRSF1B peaked at 4 hpf, strongly decreased at 7 hpf and then remained low. In situ hybridization corroborated RT-qPCR analyses and, additionally, showed that both TNFRs were ubiquitously expressed in zebrafish embryos (supplementary material Fig. S2B). In addition, mRNA for TNFα was first detected 24 hpf and increased after 72 hpf (supplementary material Fig. S2A), suggesting that other ligands beside TNFα might be signaling through these receptors early in development. Lymphotoxin α (LTα), which is able to bind both TNFRs in mammals (Schneider et al., 2004), would be a plausible candidate for signaling through TNFRs in early embryos because it was found to be expressed and peaked as early as 7 hpf (supplementary material Fig. S2A).

In zebrafish, one important intra-embryonic primitive hematopoiesis site is conformed by the intermediate cell mass (ICM), equivalent to the mammalian yolk sac blood island and located in the trunk ventral to the notochord. Subsequently, the definitive hematopoietic stem cells emerge from the ventral wall of the dorsal aorta and then migrate to the posterior region in the tail called the caudal hematopoietic tissue (CHT). Hematopoiesis starts at around 18 hpf in the ICM, where cells within this site differentiate into the endothelial cells of the trunk vasculature and proerythroblasts, which begin to enter the circulation at around 24 hpf (de Jong and Zon, 2005; Paik and Zon, 2010). Initially, one unique dorsal vessel is formed that will generate the dorsal aorta (DA) and caudal artery (CA). By sprouting of cells from the DA, intersegmental primary vessels (IPVs) appear anterior, and the posterior cardinal vein (PCV) and caudal vein (CV) appear posterior (Isogai et al., 2001). During a second dorsal sprouting from the PCV and CV, the functional fate of the IPVs of the primary vascular network varies according to whether or not a functional connection is made to a secondary sprout. Thus, approximately half of the IPVs eventually become part of intersegmental veins (ISVs), whereas the remainders give rise to intersegmental arteries (ISAs) (Isogai et al., 2001) (Fig. 1A).

Depletion of TNFRSF1B by a morpholino (MO) antisense oligonucleotide targeting the intron-1–exon-2 boundary of pre-mRNA (supplementary material Fig. S3 and Table S1) resulted in viable zebrafish for up to 7 days post-fertilization (dpf) with no obvious developmental delay (supplementary material Table S2). However, less than 5% of fish in all experiments showed altered head development, delayed yolk reabsorption and pericardial edema at 54 and 72 hpf compared with fish injected with a standard control MO (Fig. 1B,C). Analysis of double transgenic *fli1a*:eGFP/*gata1*:dsRed fish to visualize in vivo blood vessel formation (endothelial cells stained green) and circulation (erythrocytes stained red) revealed that TNFRSF1B depletion resulted in the absence of blood circulation and erythrocyte accumulation within the DA and CA at 54 hpf (Fig. 1B) and the appearance of large hemorrhages throughout the body, blood pooling and aberrant CV formation at 72 hpf (Fig. 1C-F). Although IPV formation was largely unaffected, abnormal non-functional and

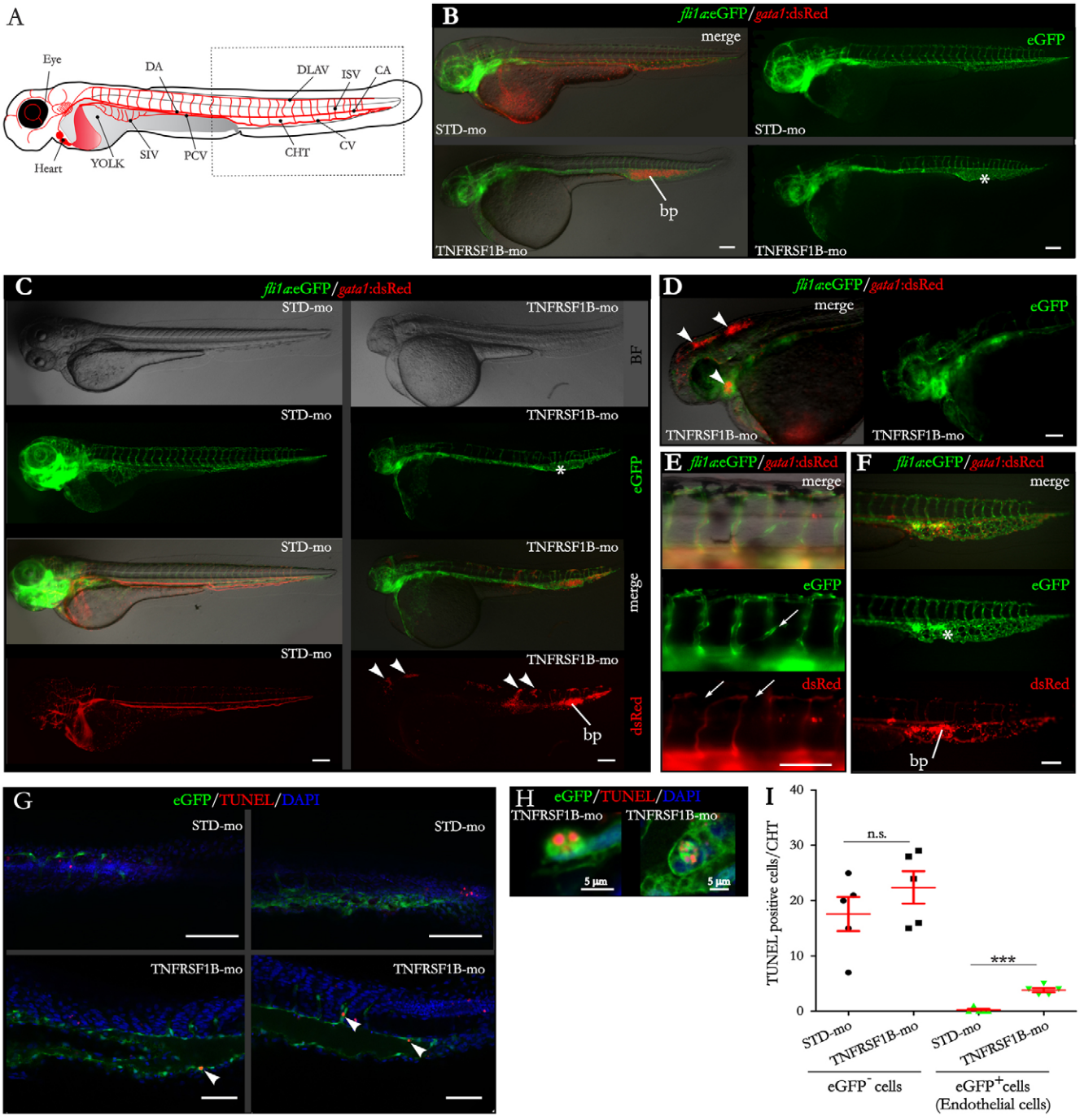

Fig. 1. Genetic depletion of TNFRSF1B results in endothelial cell apoptosis and blood circulation disruption. (A) Scheme showing the main vessels of a 3-day-old zebrafish larvae. (B-G) Lateral view of 54 (B) and 72 (C-F) hpf and tranverse and sagittal sections (G, bottom panels) of double transgenic *fli1a*:eGFP and *gata1*:dsRed larvae microinjected at the one-cell stage with standard control (STD-mo) and TNFRSF1B MOs. (B) TNFRSF1B depletion results in impaired differentiation of the CA and CV during the first sprouting, leading to blood pooling (bp) inside an enlarged unique dorsal vessel (asterisk). (C,D) At 72 hpf, blood pooling can still be observed in the caudal body part. In addition, hemorrhages appear throughout the body (arrowheads). (E,F) Zoomed views of trunk vasculature of 72 hpf larvae. TNFRSF1B deficiency results in the alteration of the second sprouting leading to the formation of a net of vessels that replace the CA and CV (E,F) and altered development of ISV (E). Arrows indicate ISA without blood circulation. (G,H) Confocal Z-stack sections of whole larvae (G) and sections (H) of the CHT of 60 hpf Tg(*fli1a*:eGFP) injected with standard and TNFRSF1B MOs showing TUNEL-positive cells (red) (arrowheads). Nuclei were counterstained with DAPI (blue). (I) Quantification of TUNEL-positive non-endothelial cells ($eGFP^{-}$) and endothelial cells ($eGFP^{+}$) at 60 hpf from serial Z-stack sections. Each dot represents the number of TUNEL-positive cells per single larvae. The mean ± s.e.m. of the TUNEL-positive cells for each group of larvae is also shown; ***P<0.001. Scale bars: 100 µm unless otherwise indicated. CA, caudal artery; CV, caudal vein; CHT, caudal haematopoietic tissue; DA, dorsal aorta; DLAV, dorsal longitudinal anastomotic vessel; IPV, intersegmental primary vessels; ISV, intersegmental vessels; PCV, posterior cardinal vein; SIV, subintestinal vessels.

bypassed ISVs and ISAs were observed (Fig. 1E). These defects resulted in a caudal vessel net with or without blood circulation (Fig. 1F). In addition, we found increased numbers of TUNEL-positive endothelial cells in TNFRSF1B-deficient embryos, whereas there were no statistically significant differences in the numbers of TUNEL-positive non-endothelial cells between control and TNFRSF1B-deficient larvae (Fig. 1G,H). These results suggest that apoptosis of endothelial cells was largely responsible for the vascular defects triggered by TNFRSF1B depletion.

The vascular defects observed in TNFRSF1B-deficient larvae were also found with two additional MOs (supplementary material Table S1), which targeted the exon-1–intron-1 boundary and the ATG–5 UTR (supplementary material Fig. S4). The defects were also rescued by the overexpression of wild-type *TNFRSF1B* mRNA but not by antisense *TNFRSF1B* mRNA (Fig. 2A). In addition, to further confirm the specificity of these MOs, we generated a dominant-negative mutant of TNFRSF1B (DN TNFRSF1B) and expressed the mRNA in embryos. DN TNFRSF1B lacks the entire intracellular signaling domain, but is identical to full-length TNFRSF1B in its transmembrane and extracellular domains. Trimerization of DN TNFRSF1B with endogenous TNFRSF1B is expected to extinguish TNFRSF1B signaling (Fang et al., 2008). Hence, it was found that overexpression of the mRNA of DN TNFRSF1B resulted in similar vascular defects; although the phenotype was less penetrating and hemorrhages were less frequent (supplementary material Fig. S5). Strikingly, although TNFRSF1A knockdown (supplementary material Fig. S3) had no effect on vascular development, it was able to rescue the vascular defect observed in TNFRSF1B-deficient embryos (Fig. 2B), further confirming the specificity of the MOs used.

Pharmacological and genetic manipulation of NF-κB has shown that NF-κB signaling via TNFRs is involved in endothelial cell survival (Santoro et al., 2007), therefore we overexpressed NEMO, which is the regulatory subunit of the IκB kinase and is required for NF-κB activation. NEMO was able to rescue in a dose-dependent manner the wild-type vascular phenotype in TNFRSF1B-deficient fish (Fig. 2C). Notably, TNFRSF1B deficiency also resulted in the induction of TNFRSF1A and TNFα gene expression, which was fully rescued by the depletion of TNFRSF1A (Fig. 2D). These results suggest that the depletion of TNFRSF1B results in an imbalance between TNFRSF1A and TNFRSF1B signaling, which, in turn, results in the activation of an apoptotic pathway through TNFRSF1A, leading to endothelial cell death, vasculature disruption and/or hemorrhages.

TNFRSF1B depletion triggers a caspase-8 apoptotic pathway via TNFRSF1A in endothelial cells

Because caspase-8 is the main initiator caspase involved in TNFR signaling, we analyzed caspase-8 activity in TNFRSF1B-deficient fish. Fig. 3A shows that the depletion of TNFRSF1B not only increased caspase-8 activity, but also increased that of caspase-9, an initiator caspase of the intrinsic apoptotic pathway that is usually activated following mitochondrion architecture demolition (Taylor et al., 2008). Genetic depletion of caspase-8 with specific MOs (Sidi et al., 2008) and the inhibition of caspase-8 by overexpression of the mRNA of the specific inhibitors CASP8 and FADD-like apoptosis regulator (CFLAR) and cytokine response modifier A (CRMA), which are zebrafish endogenous and cowpox virus caspase-8 inhibitors, respectively, resulted in a partial rescue of the vascular defect promoted by TNFRSF1B deficiency (Fig. 3B,C). However, caspase-9 depletion was unable to rescue the vascular defect of TNFRSF1B-deficient embryos (Fig. 3D). As the caspase-9 MO is not 100% efficient (Sidi et al., 2008), we cannot rule out an involvement of caspase-9 in the vascular defects observed in the TNFRSF1B morphant. Collectively, these data suggest the activation of an apoptotic pathway, initiated by caspase-8 via TNFRSF1A, that promotes endothelial cell apoptosis in the absence of NF-κB-dependent survival signals provided by TNFRSF1B activation.

P53 activation is indispensable for promoting caspase-8-dependent apoptosis of endothelial cells in TNFRSF1B-deficient zebrafish embryos

The activation of caspase-9 in TNFRSF1B-deficient embryos led us to look more closely at the contribution of the intrinsic apoptotic pathway in vascular development and maintenance. We observed the induction of P53 at both mRNA (Fig. 4A) and protein (Fig. 4B,C) levels in TNFRSF1B-deficient zebrafish. Strikingly, P53 was mainly induced in endothelial cells (Fig. 4C), which further suggests that TNFR signaling plays a crucial role in vascular development. Furthermore, the induction of P53 observed in TNFRSF1B-deficient embryos was strongly reduced in embryos deficient in both TNFRSF1A and TNFRSF1B. The induction was caspase-8-dependent because genetic depletion of caspase-8 largely attenuated P53 induction (Fig. 4A). Finally, the activation of P53 was also confirmed by the sharp upregulation of the P53-dependent genes encoding BAX and MDM2 (Fig. 4D) and P21 (Fig. 4E) in TNFRSF1B-deficient embryos.

To clarify the importance of P53 induction and activation in vascular integrity, we depleted P53 by using a specific MO (Langheinrich et al., 2002) and used the P53 zebrafish mutant line P53M214K (Berghmans et al., 2005). We found that the P53 MO almost completely rescued the vascular defects of TNFRSF1B-deficient embryos (Fig. 4F) and abrogated the induction of caspase-8 gene expression (Fig. 4G). Similarly, the P53M214K mutant embryos did not show significant vascular alteration (data not shown) and P21 and caspase-8 gene expression was unaltered (Fig. 4H) following genetic depletion of TNFRSF1B. Strikingly, however, TNFRSF1B deficiency in this line resulted in caspase-8 activation, although caspase-9 activity was unaltered (Fig. 3A). Collectively, these results suggest the re-amplification of TNFRSF1A-dependent apoptosis of endothelial cells by a crosstalk between extrinsic (caspase-8) and intrinsic (P53) apoptotic pathways (Fig. 4I).

DNA fragmentation in endothelial cells triggers P53 activation in TNFRSF1B-deficient zebrafish

Because caspase-activated deoxyribonuclease (CAD) is an endonuclease that is activated once caspases cleave its inhibitor (ICAD) and because TNFRSF1B depletion results in DNA fragmentation in endothelial cells, we overexpressed zebrafish ICAD in TNFRSF1B-deficient embryos. We found that ICAD overexpression rescued the vascular defects of TNFRSF1B-deficient embryos in a dose-dependent manner (Fig. 5A) and reduced (by about 25%) the induction of caspase-8 and P53 (data not shown). We next asked whether the checkpoint kinase CHK1 might be involved in the activation of P53 following CAD-mediated DNA damage. To inhibit CHK1, we used the indolocarbazole small

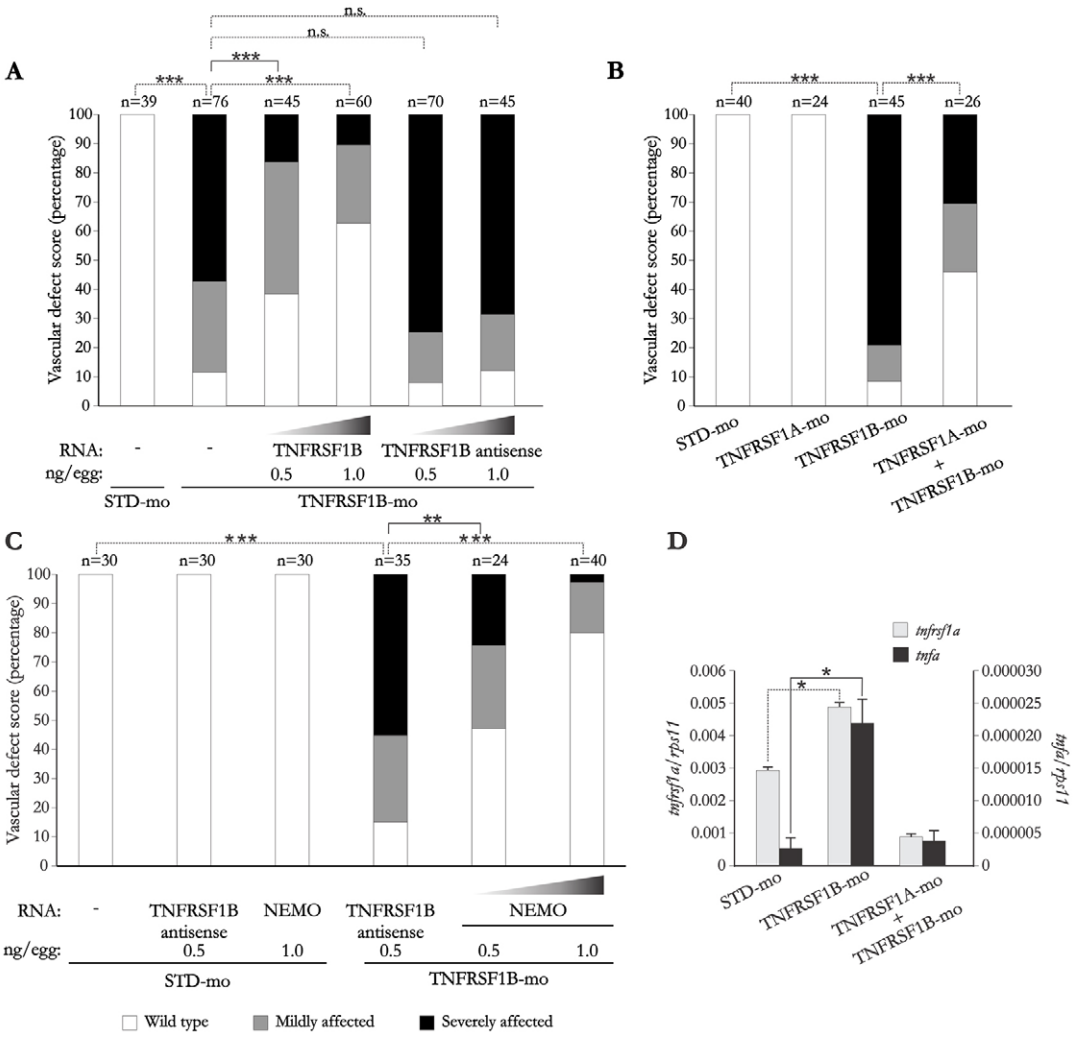

Fig. 2. A crucial balance between TNFRSF1A and TNFRSF1B signaling is required for endothelial cell development and maintenance. (A-D) Zebrafish embryos were microinjected at the one-cell stage with standard (STD-mo) and TNFRSF1B MOs alone or in combination with the indicated mRNAs. At 72 hpf, the vascular defects were scored. Larvae revealing no defects were scored as wild type (white), larvae showing erythrocyte accumulation in the CHT, partial blood circulation and hemorrhages were scored as mildly affected (gray) and larvae displaying erythrocyte accumulation in the CHT and no blood circulation as severely affected (black). (A) Effect of wild-type and antisense *TNFRSF1B* mRNA overexpression in morphant embryos. Note that wild-type, but not antisense *TNFRSF1B* mRNA partially rescues the TNFRSF1B morphant phenotype (B) Partial rescue of the vascular defect promoted by genetic depletion of TNFRSF1B by TNFRSF1A depletion. (C) NEMO-mediated activation of NF-κB partially rescues the vascular defect promoted by genetic depletion of TNFRSF1B. (D) mRNA quantification of the indicated genes were determined by real-time RT-PCR in 10 pooled larvae. The gene expression is normalized against *rps11* and are representative of two independent experiments. Each bar represents the mean + s.e.m.; **P*<0.05, ***P*<0.01, ****P*<0.0001; n.s., not significant according to Chi-square contingency (A-C) or Student's *t*-tests (D).

molecule Gö6976, which has a high specificity for CHK1 and has been successfully used in whole zebrafish embryos (Sidi et al., 2008). Genetic depletion of P53 failed to rescue the vascular defects of TNFRSF1B-deficient embryos in the presence of Gö6976 (Fig. 5B), suggesting that CHK1 might be downstream of P53 in this apoptotic signaling pathway triggered by TNFRSF1A in endothelial cells.

TNFRSF1A apoptotic signaling pathway is independent of caspase-3 but requires caspase-2

To identify the executor caspase linking the TNFRSF1A–caspase-8 and CAD–P53 axis, we analyzed the activation of caspase-3, which is a hallmark of both extrinsic and intrinsic apoptotic pathways. Interestingly, although TNFRSF1B depletion resulted in increased numbers of apoptotic endothelial cells in the CHT (Fig. 1I,J), it failed to significantly increase active caspase-3 levels in endothelial cells compared with control embryos (injected with a standard MO) (Fig. 6A). Because CAD is involved in the TNFRSF1A apoptotic signaling pathway of zebrafish endothelial cells, we studied the involvement of caspase-2, which has been shown to process ICAD (Dahal et al., 2007) and is involved in an apoptotic response to DNA damage that bypasses caspase-3 (Sidi et al., 2008). We found that caspase-2 is activated in TNFRSF1B-deficient embryos and seems to be placed downstream of caspase-8 because genetic depletion of caspase-8 reduced caspase-2

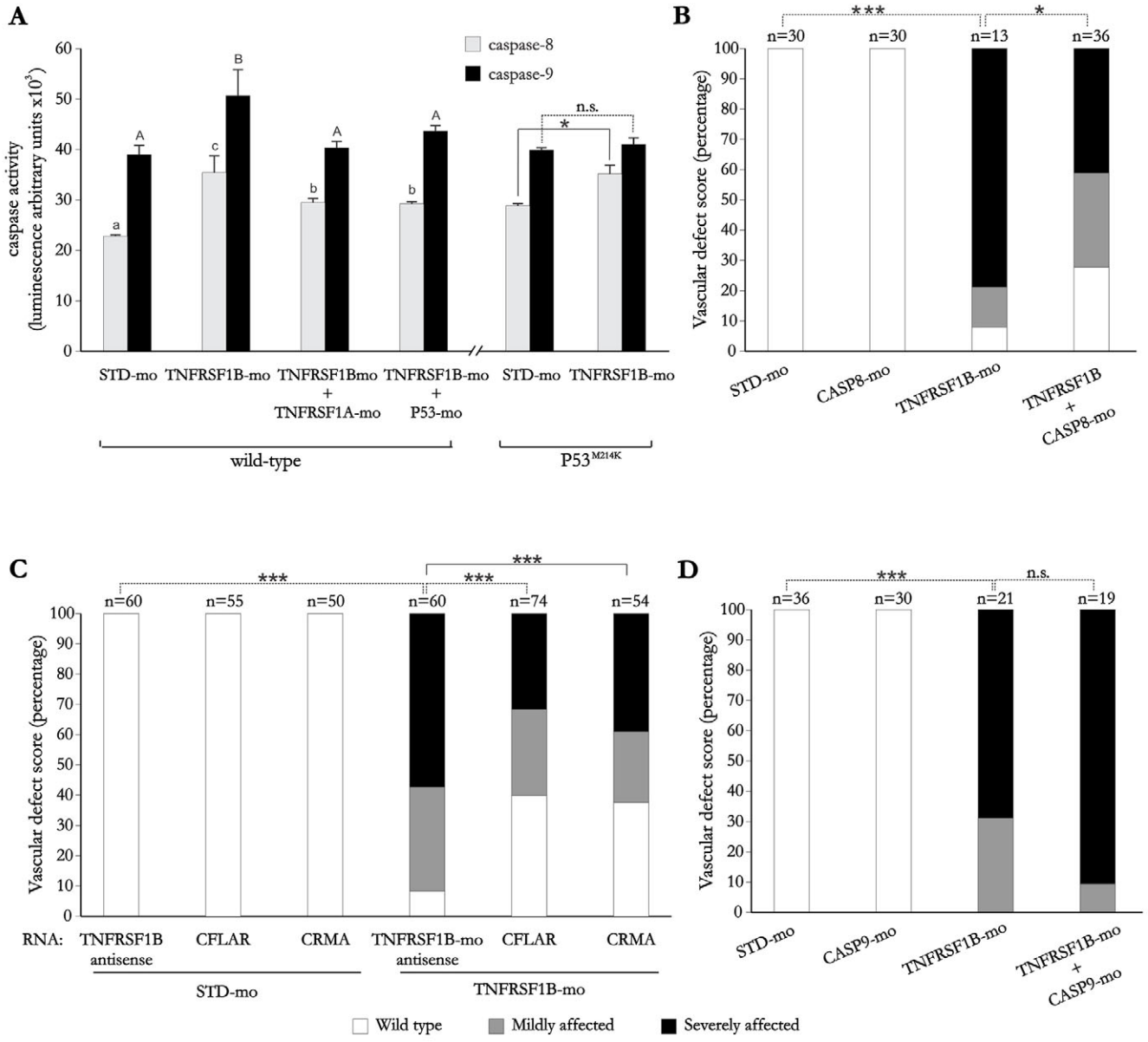

Fig. 3. TNFRSF1B depletion promotes a caspase-8 apoptotic pathway via TNFRSF1A in endothelial cells. (A-D) Wild-type and P53^{M214K} zebrafish embryos were microinjected at the one-cell stage with standard, TNFRSF1A, TNFRSF1B, P53, CASP8 and CASP9 MOs alone or in combination with the mRNAs encoding the caspase-8 inhibitors CFLAR and CMRA. (A) The activation of caspase-8 and caspase-9 in whole embryos was quantified at 60 hpf using the luminescent assays Caspase-Glo 8 and Caspase-Glo 9. Represented are mean values + s.e.m. (B-D) Vascular defects scored at 72 hpf as indicated in the legend to Fig. 2. Different letters denote statistically significant differences among the groups according to a Tukey test. Note that inhibition of the caspase-8 but not caspase-9 pathway partially rescues the TNFRSF1B vascular phenotype. *P<0.05, **P<0.01, ***P<0.0001; n.s., not significant according to a Chi-square contingency test (B-D).

activation in TNFRSF1B-deficient animals (Fig. 6B). To corroborate the relevance of caspase-2 activation in endothelial cell apoptosis, we ablated caspase-2 using a specific MO (Sidi et al., 2008). The results showed that caspase-2 deficiency was able to partially rescue the vascular defects of TNFRSF1B-deficient embryos (Fig. 6C).

Caspase-2–P53 apoptotic signaling pathway triggered by TNFRSF1A is evolutionarily conserved

We next wondered whether this new signaling pathway also operates in human endothelial cells. We first confirmed by RT-PCR that primary human umbilical vein endothelial cells (HUVECs) expressed both TNFRs (data not shown). Treatment of primary HUVECs with recombinant TNFα resulted in the induction of apoptosis in a small proportion of cells (ranging from 10-20%) (Fig. 7A-C), whereas the neutralization of TNFRSF1B with a specific antibody slightly increased the percentage of cells undergoing apoptosis in response to TNFα (Fig. 7A). More importantly, the numbers of caspase-2-positive cells significantly increased (Fig. 7B), whereas caspase-3 levels hardly increased following treatment of the cells with a TNFα mutein that

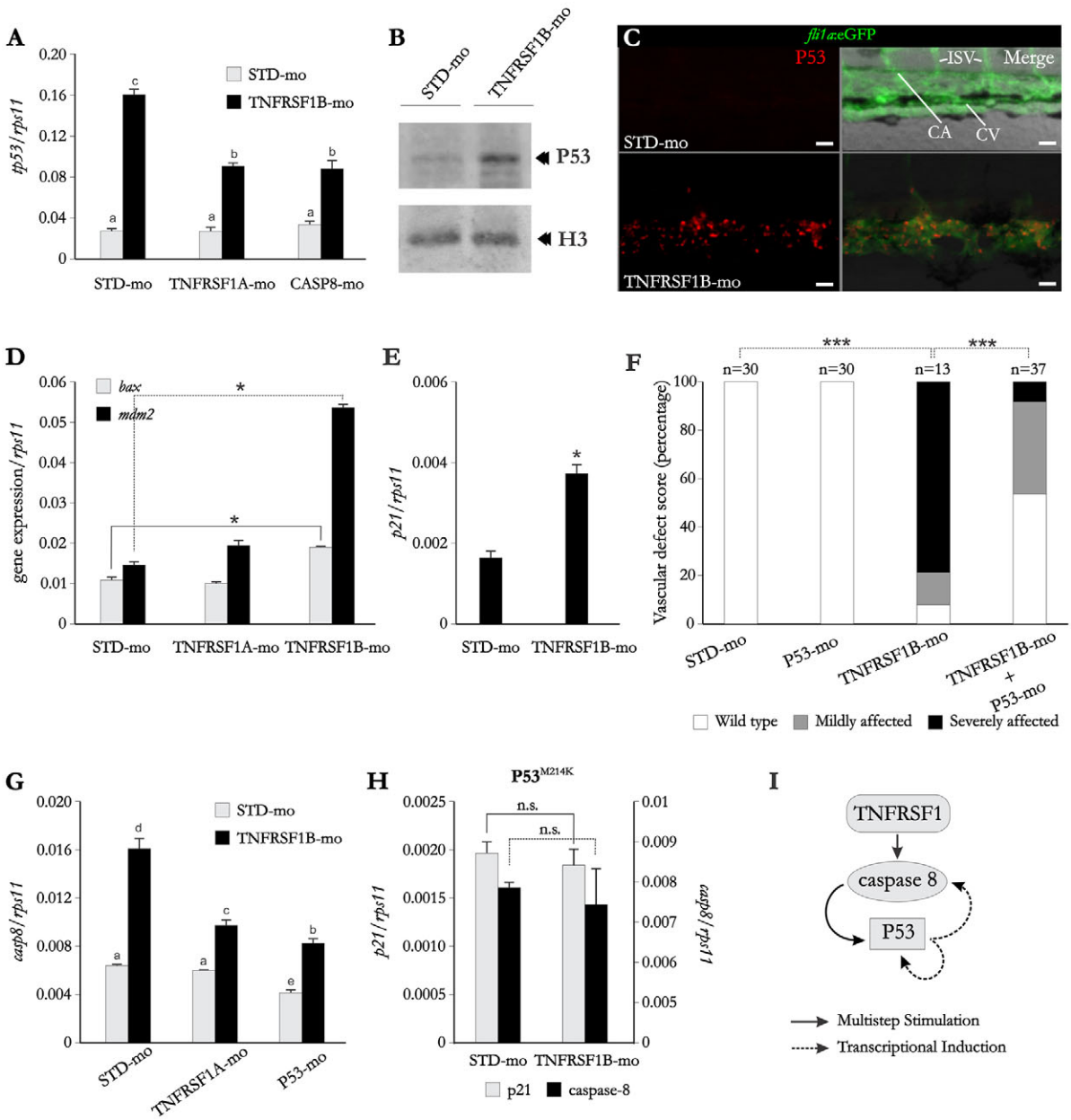

Fig. 4. P53 activation is indispensable for promoting caspase-8-dependent apoptosis of endothelial cell in TNFRSF1B-deficient zebrafish. (A-H) Wild-type (A,B,D-G), transgenic *fli1a*:eGFP (C) and P53^{M214K} (H) zebrafish embryos were microinjected at the one-cell stage with standard, TNFRSF1A, TNFRSF1B and P53 MOs. At 72 hpf, the mRNA levels of the indicated genes were determined by real-time RT-PCR in 10 pooled larvae (A,D,E,G,H). The gene expression is normalized against *rps11*, each bar represents the mean + s.e.m. Different letters denote statistically significant differences among the groups according to a Tukey test. *P<0.05; n.s., not significant according to Chi-square contingency (F) or Student's t tests (D,E,H). (A) Co-injection of TNFRSF1A or CASP8 MOs reduces TNFRSF1B-MO-mediated P53 upregulation. (B) P53 protein levels were assayed by western blot in dechorionated and deyolked embryos at 24 hpf. Note that P53 levels are upregulated in TNFRSF1B-deficient larvae. (C) Whole mount immunohistochemistry against P53 at 3 dpf in Tg(*fli1a*:eGFP) larvae injected with standard or TNFRSF1B MOs. Note a massive increase in P53 expression (red) in the vascular endothelium (green) of TNFRSF1B-deficient larvae. (D,E) TNFRSF1B silencing leads to upregulation of *bax*, *mdm2* and *p21*. (F) Vascular defects in larvae deficient in both TNFRSF1B and P53 were scored as indicated in the legend to Fig. 2. Note that P53 deficiency partially rescues the vascular defects observed in TNFRSF1B-deficient fish. (G) Upregulation of caspase-8 by TNFRSF1B deficiency is dependent on TNFRSF1A and P53. (H) *p21* mRNA levels in P53 mutant larvae are not altered by TNFRSF1B silencing. (I) Representation of the proposed amplification loop between extrinsic and intrinsic apoptotic pathways triggered by TNFRSF1A. CA, caudal artery; CV, caudal vein; ISV, intersegmental vessels. Scale bars: 25 μm.

specifically interacts with TNFRSF1A (Fig. 7D). In addition, levels of mRNAs encoding P21 and P53 also increased following treatment with TNFα mutein (Fig. 7E) and, notably, pharmacological inhibition of CHK1 with Gö6976 resulted in a further upregulation of P53 and P21 gene expression (Fig. 7E) and accumulation of P53 protein (Fig. 7F). These results suggest

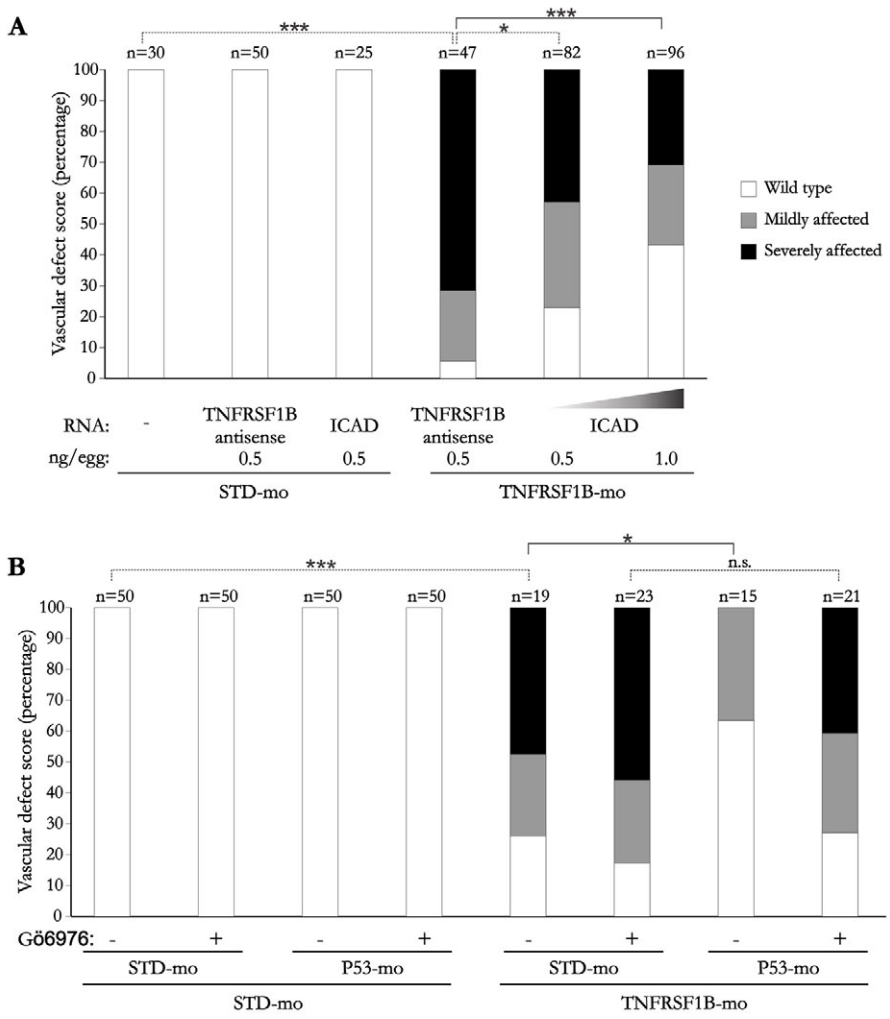

Fig. 5. DNA fragmentation in endothelial cells triggers P53 activation in TNFRSF1B-deficient zebrafish. (A,B) Wild-type zebrafish embryos were microinjected at the one-cell stage with standard and/or TNFRSF1B MOs alone or in combination with the mRNAs encoding ICAD or the antisense mRNA for TNFRSF1B, as an appropriate control. Some larvae were treated at 48 hpf by bath immersion for 16 hours with 1 μM of the CHK1 specific inhibitor Gö6976. Vascular defects were scored at 72 hpf as indicated in the legend to Fig. 2. **P*<0.05, ***P*<0.01, ****P*<0.0001; n.s., not significant according to a Chi-square contingency test.

that this kinase is involved in a P53- and P21-dependent cell cycle arrest triggered by TNFRSF1A in endothelial cells.

DISCUSSION

Tight molecular control of endothelial cell survival, integrity and apoptosis is essential for both embryonic and adult angiogenesis. Santoro and coworkers recently showed that the anti-apoptotic adaptor protein BIRC2 plays an essential role in regulating endothelial cell survival in vivo (Santoro et al., 2007). However, because BIRC2 is known to be involved in the signaling pathways of several death receptors, including FAS (Ruemmele et al., 2002), CD40 (Bureau et al., 2002; Fotin-Mleczek et al., 2002), TNFRSF1A (Shu et al., 1996) and TNFRSF1B (Rothe et al., 1995), the nature of the receptor(s) involved in vascular development and integrity remains unclear. Using a gain- and loss-of-function approach, we found that the TNFRSF1A and TNFRSF1B signaling pathways must be balanced for endothelial cell development to be maintained in zebrafish. Furthermore, in endothelial cells, TNFRSF1A signals apoptosis through complex II and caspase-8, whereas TNFRSF1B signals survival via complex I and NF-κB. A similar crosstalk between TNFRSF1A and TNFRSF1B signaling pathways has also been observed in human aortic endothelial cells, whose susceptibility to TNFα treatment can be rescued by blocking TNFRSF1A or NF-κB (Okada et al., 2001). These results, together with the ability of TNFRSF1B to induce the depletion of TRAF2 and BIRC2 proteins and accelerate the TNFRSF1A-dependent activation of caspase-8 (Fotin-Mleczek et al., 2002), suggest that BIRC2 is required for TNFRSF1B complex I formation and NF-κB activation in endothelial cells, despite the high promiscuity of this adaptor molecule.

One of the most interesting observations made in our study is that the TNFRSF1A-dependent apoptotic pathway of endothelial cells is independent of caspase-3 and caspase-9, but requires caspase-2, an enigmatic caspase that possesses both initiator and executioner caspase characteristics (Krumschnabel et al., 2009). Our in vivo epistasis analysis led us to envisage a model whereby TNFRSF1A engagement leads to the following sequential events (Fig. 8): (i) activation of caspase-8, (ii) activation of caspase-2, (iii) processing of ICAD by caspase-2 and translocation of CAD to the nucleus, (iv) activation of P53, and (v) P53-dependent induction of caspase-8 gene expression. As human caspase-2 has been shown to cleave ICAD in vitro (Dahal et al., 2007), we hypothesised that caspase-2 would replace caspase-3 as the main executor caspase and would mediate the cleavage of ICAD and the subsequent activation of P53. In fact, we observed that P53 was firmly involved in the TNFRSF1A-mediated apoptosis of endothelial cells.

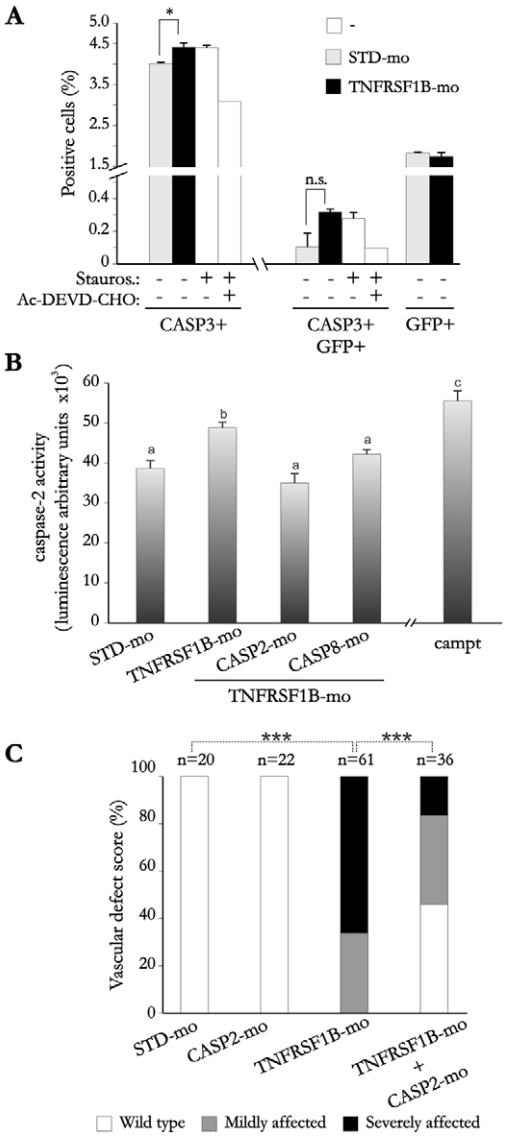

Fig. 6. The TNFRSF1A apoptotic signaling pathway of endothelial cells is independent of caspase-3 but requires caspase-2. (A-C) Wild-type and transgenic *fli1a*:eGFP zebrafish embryos were microinjected at the one-cell stage with standard, TNFRSF1B, CASP8 and/or CASP2 MOs. (A) The activation of caspase-3 in embryos was quantified at 60 hpf by flow cytometry using a specific antibody for active caspase-3. (B) Caspase-2 levels were determined using the luminescent assay Caspase-Glo 2. (C) Vascular defects were also scored at 72 h.p.f. as indicated in the legend to Fig. 2. Note that TNFRSF1B depletion resulted in the caspase-8 dependent activation of caspase-2 and that caspase-2 depletion rescued the vascular defects of TNR2-deficient fish. Some larvae were treated at 48 hpf by bath immersion for 16 hours with 0.5 μM camptothecin (campt) or 0.5 μM staurosporine (Stauros) in the presence or absence of 100 μM of the caspase-3 inhibitor Ac-DEVD-CHO, as appropriate controls for caspase activation. Different letters denote statistically significant differences between the groups according to a Tukey test; **P*<0.05, ****P*<0.0001; n.s., not significant, according to Student's *t*-test (A) and Chi-square contingency test (C).

Furthermore, P53 might also be involved in the direct activation of caspase-2 in TNFRSF1B-deficient endothelial cells, as indicated by recent findings that that caspase-2 is involved in a P53-positive feedback loop during DNA damage response (Oliver et al., 2011). Thus, caspase-2 cleaves MDM2, promoting P53 stability, which leads to the transcription of PIDD, a P53 target gene product that activates caspase-2 in a complex called the caspase-2–PIDDosome. Regardless of the mechanism, the apoptotic program triggered by TNFRSF1A in endothelial cells involves a positive regulatory feedback between the intrinsic and extrinsic apoptotic pathways, which ends in the upregulation of caspase-8, further contributing to the apoptosis of endothelial cells. To the best of our knowledge, this observation has not previously been reported in vivo but it is not unexpected because P53 has also been found to be able to upregulate caspase-8 gene transcription in human cancer cells treated with cytotoxic drugs (Ehrhardt et al., 2008).

The inhibition of the cell cycle checkpoint kinase CHK1, which is activated by ATR in response to replication stress (Cuadrado et al., 2006), impairs the ability of P53 knockdown to rescue the vascular defect promoted by TNFRSF1A in zebrafish embryos and further induces the expression of P21 in TNFα-treated HUVECs, indicating that CHK1 might be downstream of P53 in the apoptotic signaling pathway triggered by TNFRSF1A in endothelial cells or, alternatively, it might inhibit a P53-independent apoptotic pathway in these cells. This is not unexpected because a role for CHK1 has recently been described in the inhibition of an ATM/ATR–caspase-2 apoptotic response to irradiation-induced DNA damage that bypasses P53 and caspase-3 (Sidi et al., 2008). Although the CHK1-dependent and P53-independent apoptotic pathway triggered by TNFRSF1A deserves further investigation, our results also suggest that CHK2 mediates activation of P53 in TNFRSF1B-deficient endothelial cells.

Although several systemic inhibitors of TNFα, such as soluble TNF receptors and anti-TNFα antibodies, have been approved for the treatment of human diseases where TNFα plays a pathogenic role, these drugs exhibit severe side effects and are expensive. Hence, new active blockers of TNFα that are safe, efficacious and inexpensive are urgently needed (Sethi et al., 2009). We believe that the TNFRSF1A apoptotic axis described in this study reveals new molecular targets for the development of therapeutic drugs for human diseases where TNFα plays a major role, such as inflammatory and autoimmune disorders, ischemia-reperfusion injury and cancer. The TNFα-induced caspase-2–P53 apoptotic program in HUVECs, the vascular defects of TNFRSF1A-deficient zebrafish and the recent observations in transgenic mice overexpressing TNFRSF1B in endothelial cells showing decreased death of these cells after ischemia-reperfusion and higher endothelial cell proliferation, neovascularization and vessel maturation after injury (Luo et al., 2010), strongly suggest that TNFRSF1A and TNFRSF1B, rather than TNFα, might be the better clinical targets.

In conclusion, we have identified an evolutionarily conserved apoptotic program in endothelial cells that is triggered by the imbalance between survival and death signals provided by TNFRs. This pathway involves crosstalk between intrinsic (caspase-8) and extrinsic (P53) apoptotic programs but, intriguingly, bypasses caspase-3. Caspase-2 replaces caspase-3 and links both apoptotic programs, probably due to its dual activity as initiator and executor caspase. This genetic pathway reveals new therapeutic targets for the control of inflammation- and tumor-induced angiogenesis.

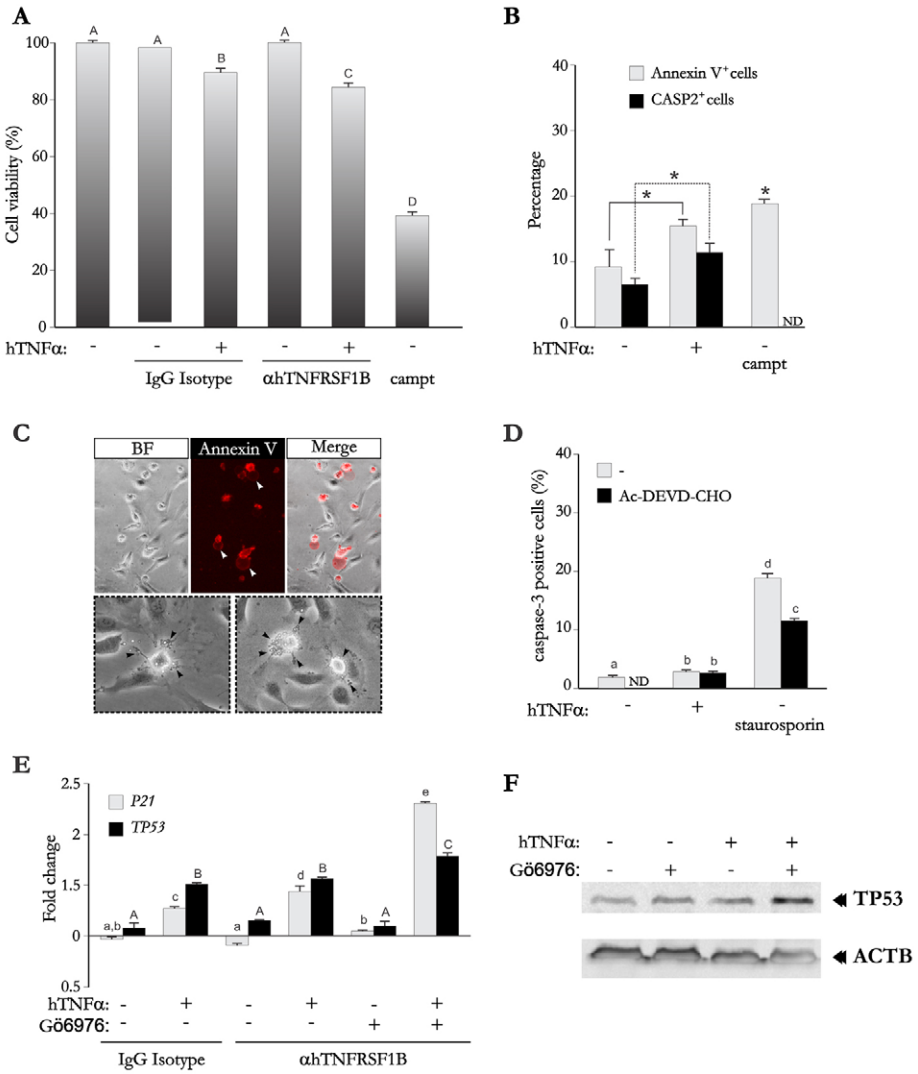

Fig. 7. The caspase-2–P53 apoptotic signaling pathway triggered by TNFRSF1A is evolutionarily conserved. (A-F) HUVEC were treated for 16 hours with 40 ng/ml human TNFα (hTNFα) alone or in combination with 5 μg/ml of a mouse IgG isotype control or a neutralizing antibody to human TNFRSF1B (αhTNFRSF1B) (A,E) or with a TNFα mutein specific for TNFRSF1A (B-D,F). (A) Cell viability was determined using the MTT colorimetric assay. (B,C) PS flip and caspase-2 activity were evaluated by flow cytometry and immunofluorescence using phycoerythrin-Annexin V conjugate and the CaspGLOW Fluorescein Active Caspase-2 Staining kit, respectively. Note that Annexin V$^+$ cells showed membrane blebbing (C, arrowheads). BF, bright field. (D) Caspase-3 activation was determined by immunofluorescence using a specific antibody to active caspase-3. Some cultures were treated for 16 hours with 0.5 μM camptothecin (campt), 1 μM Gö6976 or 0.5 μM staurosporine in the presence or absence of 50 μM of the caspase-3 inhibitor Ac-DEVD-CHO. (E) mRNA levels of the indicated genes were determined by real-time RT-PCR, normalized against *rps11*, and shown relative to non-treated cells (mean + s.e.m.). (F) P53 protein levels were assayed by western blot using monoclonal antibodies to human P53 (TP53) and β-actin (ACTB). Different letters denote statistically significant differences between the groups according to a Tukey test. The groups labeled with 'a' or 'A' in E were not statistically significant from non-treated cells. *P<0.05 according to a Student's t-test; ND, not determined.

MATERIALS AND METHODS

Animals

Wild-type zebrafish (*Danio rerio* H. Cypriniformes, Cyprinidae) were obtained from the Zebrafish International Resource Center (ZIRC) and maintained as described in the zebrafish handbook (Westerfield, 2000). The transgenic zebrafish line that expresses enhanced GFP (eGFP) driven by the endothelial cell-specific promoter *fli1a* gene *Tg(fli1a:egfp)y1* (Lawson and Weinstein, 2002) was obtained from ZIRC. The transgenic line with red fluorescent erythrocytes *Tg(gata1:dsRed)sd2* (Traver et al., 2003) and the P53 mutant line *zdf1* (P53^{M214K}) (Berghmans et al., 2005) were kindly provided by Leonard I. Zon (HSCRB, Harvard University, Cambridge, MA). The experiments described comply with the Guidelines of the European Union Council (86/609/EU) and of the Bioethical Committee of the University of Murcia (approval number #333/2008) for the use of laboratory animals.

Embryos and larvae were anesthetized in Tricaine (200 μg/ml) and examined using a Leica MZ16FA stereomicroscope. The vascular defects were scored semiquantitatively in blind samples at 48 and 72 hpf as wild type (no defects), mildly affected (erythrocyte accumulation in the CHT, partial blood circulation and hemorrhages) and severely affected (erythrocyte accumulation in the CHT and no blood circulation).

Morpholinos, mRNA microinjection and chemical treatment

Splice- or translation-blocking MOs were designed by and purchased from Gene Tools and solubilized in water (1-3 mM) (supplementary material Table S1). All eggs were injected with the same amount of MOs. Full-length TNFRSF1A (BC068424), TNFRSF1B (ENSDARG00000070165) and ICAD (NM_001002631), and DN TNFRSF1B (amino acids 1-162) were subcloned into the pCS2+ or pBluescript II KS+ vectors. NEMO and CFLAR in a PCS2 backbone were provided by Massimo Santoro (University of Turin, Turin, Italy) (Santoro et al., 2007). CMRA construct was obtained from the BCCM/LMBP plasmid collection (Ghent University, Belgium).

mRNA was synthesized using the mMESSAGE MACHINE kit (Ambion) and polyadenylated using a polyadenylation kit (Ambion) according to the manufacturer's instructions. mRNA (0.5-1 ng/egg) and MOs (1-5 ng/egg) were mixed in microinjection buffer (0.5× Tango buffer and 0.05% phenol red solution) and microinjected (0.5-1 nl) into the yolk sac of one-cell-stage embryos

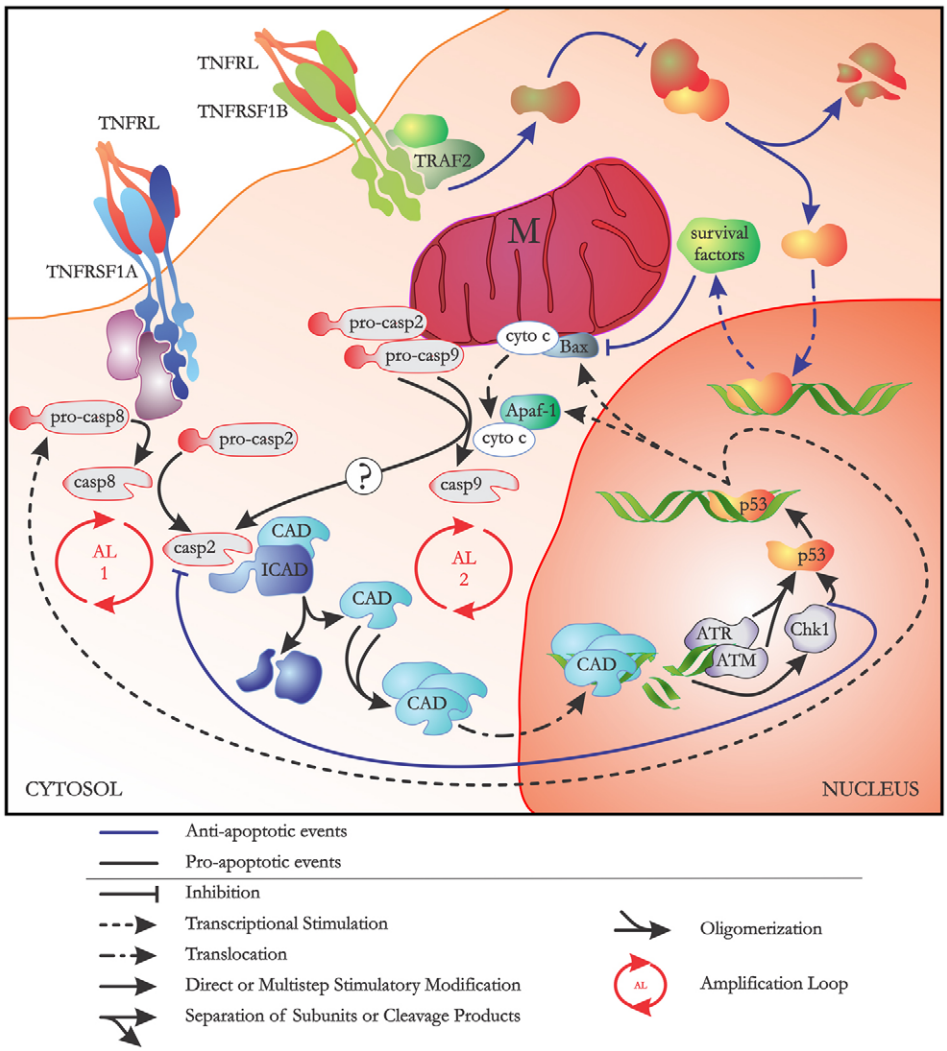

Fig. 8. Model of TNFR signaling in endothelial cells. The TNFRSF1A apoptotic and TNFRSF1B survival pathways, the main elements involved, and the crosstalk between extrinsic and intrinsic apoptotic programs. TNFRL, TNFR ligands (TNFα and LTα).

using a Narishige IM300 microinjector. Knockdown efficiencies of TNFRSF1A and TNFRSF1B MOs are shown in supplementary material Fig S2.

In some experiments, 24-hpf embryos were dechorionated and transferred to fresh E3 medium containing 1% DMSO, with or without the CHK1 inhibitor Gö6976 (1 μM; Calbiochem) (Sidi et al., 2008).

Analysis of development

The effect of MOs on development was evaluated as previously reported (Kimmel et al., 1995). Briefly, the side-to-side flexures were recorded at 22 hpf (25-26 somites stage); heartbeat, red blood cells on yolk and early pigmentation in retina and skin at 24 hpf (Prim 5 stage); head trunk angle (HTA), retina pigmented, early touch reflect and straight tail at 30 hpf (Prim 15 stage); and early motility and tail pigmentation at 36 hpf (Prim 25).

Determination of caspase activity

The activation of caspase-9, caspase-8 and caspase-2 in whole embryos was quantified using the luminescent assays Caspase-Glo 9, Caspase-Glo 8 and Caspase-Glo 2 (Promega), respectively, as described previously (Geiger et al., 2006). The substrate specificity and sensitivity to pharmacological inhibitors of zebrafish caspase-8 and caspase-9 has been found to be similar to their mammalian orthologs (Chen et al., 2001; Chiu et al., 2010; Friedrich et al., 2004; Santoro et al., 2007; Stanton et al., 2006; Wrasidlo et al., 2008). Caspase-3 activation was determined by flow cytometry using an affinity-purified rabbit anti-human/mouse caspase-3 active (0.5 μg/ml; epitope CRGTELDCGIETD, #AF835, R&D Systems) (Sepulcre et al., 2011). As appropriate controls, 56-hpf larvae were treated for 16 hours with 0.5 μM camptothecin or staurosporine (Sigma-Aldrich) in the presence or absence of the caspase-3-specific inhibitor Ac-DEVD-CHO (100 μM; Sigma-Aldrich).

Analysis of gene expression

Total RNA, extracted as indicated above, was treated with DNase I, amplification grade (1 unit/μg RNA; Invitrogen). SuperScript III RNase H$^-$ ReverseTranscriptase (Invitrogen) was used to synthesize the first strand of cDNA with an oligo-dT$_{18}$ primer from 1 μg of total RNA at 50°C for 50 minutes.

Real-time PCR was performed with an ABI PRISM 7500 instrument (Applied Biosystems) using SYBR Green PCR Core Reagents (Applied Biosystems). Reaction mixtures were incubated for 10 minutes at 95°C, followed by 40 cycles of 15 seconds at 95°C

and 1 minute at 60°C, and finally by 15 seconds at 95°C, 1 minute 60°C and 15 seconds at 95°C. For each mRNA, gene expression was normalized to the ribosomal protein S11 (*rps11*) content in each sample using the Pfaffl method (Pfaffl, 2001). In all cases, the PCR was performed with triplicate samples and repeated with at least two independent samples. The primers used are shown in supplementary material Table S3.

Whole-mount immunohistochemistry

Embryos and larvae were fixed for 2 hours in 4% paraformaldehyde (PFA) at room temperature, dehydrated in methanol-PBS solutions (25, 50, 75 and 100%, 5 minutes each) and stored in 100% methanol at −20°C. For staining, they were rehydrated in 75, 50 and 25% methanol-PBT (PBS and 0.1% Tween-20) solutions (5 minutes each), washed three times for 5 minutes in de-ionized water (dH_2O), permeabilized in cold acetone for 10 minutes at −20°C, washed again twice in dH2O (5 minutes each) and treated with blocking solution (PDT; PBS containing 0.1% Tween-20, 1% DMSO, 5% FBS and 2 mg/ml BSA) for 2 hours at room temperature. After blocking, embryos were incubated overnight at 4°C with 0.5 µg/ml affinity-purified rabbit anti-human/mouse caspase-3 active or anti-zebrafish P53 (1:200; #55915, AnaSpec) diluted in PDT, washed six times in PDT (10 minutes each), incubated for 2 hours at room temperature in PDT, incubated overnight at 4°C with a 1:1000 dilution in PDT of a phycoerythrin-conjugated secondary antibody (Invitrogen), washed five times in PBT (5 minutes each) and finally examined under a LEICA MZ16FA stereomicroscope.

In situ hybridization

Whole mount in situ hybridization was performed according to a published method (Schulte-Merker et al., 1994) with minor modifications. In situ hybridization on paraffin sections was based on a protocol developed by Mallo and co-workers (Mallo et al., 2000). Similar results were obtained with three different riboprobes against TNFRSF1A (probe 1, +64 to + 572; probe 2, +666 to +1177; full length probe, +64 to +1177) and TNFRSF1B (probe 1, +113 to +667; probe 2, +678 to +1189; full length probe, +113 to +1189). The primers used to amplify the probes are shown in supplementary material Table S3.

Detection of apoptotic cell death by TUNEL labeling

After overnight fixation in 4% PFA at 4°C, embryos were washed in PBT for five minutes and dehydrated in a graded methanol series until reaching 100% methanol. After storage at −20°C they were rehydrated gradually in PBT, washed twice for 10 minutes in PBT and digested in proteinase K (Roche) solution in PBT (10 µg/µl) at room temperature for 15 minutes. After two washes in PBT, embryos were postfixed in 4% PFA for 20 minutes. Embryos were washed again twice in PBT for 10 minutes each and endogenous biotin was blocked using the Biotin Blocking Kit (Vector, Burlingame, CA). Embryos were washed in PBT and put into equilibration buffer (Roche) for 1 hour. Embryos were subsequently incubated with the TdT reaction mix (Roche) overnight at 37°C. Reaction was stopped with washes in equilibration buffer for 3 hours at 37°C followed by three washes in PBT at room temperature. Strepavidine-Cy3 (Jackson Laboratories) was then added for 1 hour at room temperature. For concomitant GFP detection, embryos were incubated with anti-GFP antibody (Clontech, Mountain View, CA) followed by Alexa-Fluor-488-conjugated secondary antibody (Invitrogen). Embryos were washed and mounted in Vectashield supplemented with DAPI (Vector).

Methanol-fixed embryos were also embedded in paraffin, sectioned at 5 µm and processed as previously described (González-Rosa et al., 2011).

Immunoprecipitation and western blot assays

The physical interaction between zebrafish TNFα and TNFRs was analyzed by means of immunoprecipitation. Plasmid DNA was prepared using the Midi-Prep procedure (Qiagen) and transfected into HEK293 cells with LyoVec transfection reagent (Invivogen), according to the manufacturer's instructions. At 48 hours after transfection, the cells were washed twice with PBS and lysed in 200 µl lysis buffer (10 mM Tris-HCl pH 7.4, 150 mM NaCl, 1% Triton X-100, 0.5% NP-40, and a 1:20 dilution of the protease inhibitor cocktail P8340 from Sigma-Aldrich). Whole cell extracts were then mixed and incubated overnight at 4°C before being immunoprecipitated with the anti-V5 mAb (Invitrogen) and protein G Sepharose (Sigma-Aldrich). After extensive washing with lysis buffer, the resins were boiled in SDS sample buffer and the bound proteins resolved on 12% SDS-PAGE and transferred for 50 minutes at 200 mA to nitrocellulose membranes (BioRad). Blots were probed with specific antibodies to V5 or Xpress (Invitrogen) and developed with enhanced chemiluminescence (ECL) reagents (GE Healthcare) according to the manufacturer's protocol.

Extracts (10 µg) from dechorionated and deyolked embryos, obtained as indicated above for HEK293 cells, were probed with a 50% dilution of the monoclonal antibody LLzp53-9E10, which is specific to zebrafish P53 (MacInnes et al., 2008). Membranes were then reprobed with a 1:5000 dilution of a commercial rabbit antibody to histone 3 (#ab1791, Abcam) as an appropriate loading control.

HUVEC culture and treatments

Primary human endothelial cells (HUVECs) were cultured in appropriate media according to the manufacturer's protocol (Lonza). Cells were stimulated for 16 hours with 40 ng/ml recombinant TNFα (Sigma-Aldrich) alone or in the presence of 5 µg/ml TNFRSF1B neutralizing antibody (#MAB226, R&D Systems) or an isotype control (#MAB003, R&D Systems). Alternatively, a TNFα mutein specific for TNFRSF1A (GenScript) was used (Loetscher et al., 1993). In some experiments, cells were also treated with 0.5 µM camptothecin, 1 µM Gö6976 or 0.25 µM staurosporine (Sigma-Aldrich) for 16 hours in the presence or absence of 50 µM of the caspase-3 inhibitor Ac-DEVD-CHO. Cell viability was determined spectrophotometrically using an MTT-based test (Mosmann, 1983). Caspase-2 activation was determined by flow cytometry using the CaspGLOW Fluorescein Active Caspase-2 Staining Kit (Biovision) and the accompanying staining protocols. Caspase-3 activation was determined by immunofluorescence as indicated for zebrafish embryos. Phosphatidylserine exposure on the extracellular leaflet of the membrane was determined by flow cytometry using a phycoerythrin-Annexin V conjugate (ENZO Life Sciences) according to the manufacturer's instructions. Finally, P53 protein levels were evaluated by western blot using monoclonal antibodies to human P53 (#P6749) and β-actin (#A5441) (both from Sigma-Aldrich).

Statistical analysis

All experiments were performed at least three times, unless otherwise indicated. The total number of animals used is indicated above each bar in the figures. Data were analyzed by Student's *t*-test, or ANOVA and a Tukey's multiple range test to determine the differences among groups. Statistical significance was defined as $P<0.05$. The Chi-square contingency test was used to determine the differences between vascular defects scores.

ACKNOWLEDGEMENTS

We thank Inma Fuentes, Pedro J. Martínez, Eduardo Díaz and Encarnación Sánchez for excellent technical assistance, Marina Peralta-López and Claudio Badía-Careaga for assistance with in situ hybridization and TUNEL, Leonard I. Zon for the *Tg(gata1:dsRed)sd2* and the P53 mutant line *zdf1*, Massimo Santoro (University of Turin, Turin, Italy) for the NEMO and CFLAR constructs, and Jacqueline A. Lees (MIT, Cambridge, MA) for the antibody to zebrafish P53.

COMPETING INTERESTS

The authors declare that they do not have any competing or financial interests.

AUTHOR CONTRIBUTIONS

F.J.R., R.E. and V.M. designed the research; F.J.R., R.E., S.C., M.P.S., J.M.G.-R., N.M. and F.A.-P., performed research; F.J.R., R.E., S.C., M.P.S., J.M.G.-R., N.M., F.A.-P., M.L.C., J.M. and V.M. analyzed data; and F.J.R. and V.M. wrote the paper with contributions from other authors.

FUNDING

This work was supported by the Spanish Ministry of Science and Innovation [grant numbers BIO2008-01379, BIO2011-23400, CSD2007-00002 to V.M.; RYC-2006-001694 to N.M.; 05/0087, PIO6/00369 to M.L.C.; fellowship to S.C.), the Fundación Séneca-Murcia [grant numbers 04538/GERM/06 to V.M.; 08760/PI/08 to M.L.C.; fellowship to R.E.], the University of Murcia [fellowship to F.A.-P.] and the Fundación Marcelino Botín [grant to V.M.].

SUPPLEMENTARY MATERIAL

Supplementary material for this article is available at
http://dmm.biologists.org/lookup/suppl/doi:10.1242/dmm.010249/-/DC1

REFERENCES

Aggarwal, B. B. (2003). Signalling pathways of the TNF superfamily: a double-edged sword. *Nat. Rev. Immunol.* **3**, 745-756.

Berghmans, S., Murphey, R. D., Wienholds, E., Neuberg, D., Kutok, J. L., Fletcher, C. D., Morris, J. P., Liu, T. X., Schulte-Merker, S., Kanki, J. P. et al. (2005). tp53 mutant zebrafish develop malignant peripheral nerve sheath tumors. *Proc. Natl. Acad. Sci. USA* **102**, 407-412.

Bureau, F., Seumois, G., Jaspar, F., Vanderplasschen, A., Detry, B., Pastoret, P. P., Louis, R. and Lekeux, P. (2002). CD40 engagement enhances eosinophil survival through induction of cellular inhibitor of apoptosis protein 2 expression: Possible involvement in allergic inflammation. *J. Allergy Clin. Immunol.* **110**, 443-449.

Chen, S., Guttridge, D. C., You, Z., Zhang, Z., Fribley, A., Mayo, M. W., Kitajewski, J. and Wang, C. Y. (2001). Wnt-1 signaling inhibits apoptosis by activating beta-catenin/T cell factor-mediated transcription. *J. Cell Biol.* **152**, 87-96.

Chiu, C. L., Wu, J. L., Her, G. M., Chou, Y. L. and Hong, J. R. (2010). Aquatic birnavirus capsid protein, VP3, induces apoptosis via the Bad-mediated mitochondria pathway in fish and mouse cells. *Apoptosis* **15**, 653-668.

Cuadrado, M., Martinez-Pastor, B. and Fernandez-Capetillo, O. (2006). "ATR activation in response to ionizing radiation: still ATM territory". *Cell Div.* **1**, 7.

Dahal, G. R., Karki, P., Thapa, A., Shahnawaz, M., Shin, S. Y., Lee, J. S., Cho, B. and Park, I. S. (2007). Caspase-2 cleaves DNA fragmentation factor (DFF45)/inhibitor of caspase-activated DNase (ICAD). *Arch. Biochem. Biophys.* **468**, 134-139.

de Jong, J. L. and Zon, L. I. (2005). Use of the zebrafish system to study primitive and definitive hematopoiesis. *Annu. Rev. Genet.* **39**, 481-501.

Ehrhardt, H., Häcker, S., Wittmann, S., Maurer, M., Borkhardt, A., Toloczko, A., Debatin, K. M., Fulda, S. and Jeremias, I. (2008). Cytotoxic drug-induced, p53-mediated upregulation of caspase-8 in tumor cells. *Oncogene* **27**, 783-793.

Fang, L., Adkins, B., Deyev, V. and Podack, E. R. (2008). Essential role of TNF receptor superfamily 25 (TNFRSF25) in the development of allergic lung inflammation. *J. Exp. Med.* **205**, 1037-1048.

Fotin-Mleczek, M., Henkler, F., Samel, D., Reichwein, M., Hausser, A., Parmryd, I., Scheurich, P., Schmid, J. A. and Wajant, H. (2002). Apoptotic crosstalk of TNF receptors: TNF-R2-induces depletion of TRAF2 and IAP proteins and accelerates TNF-R1-dependent activation of caspase-8. *J. Cell Sci.* **115**, 2757-2770.

Friedrich, E. B., Liu, E., Sinha, S., Cook, S., Milstone, D. S., MacRae, C. A., Mariotti, M., Kuhlencordt, P. J., Force, T., Rosenzweig, A. et al. (2004). Integrin-linked kinase regulates endothelial cell survival and vascular development. *Mol. Cell. Biol.* **24**, 8134-8144.

Geiger, G. A., Parker, S. E., Beothy, A. P., Tucker, J. A., Mullins, M. C. and Kao, G. D. (2006). Zebrafish as a "biosensor"? Effects of ionizing radiation and amifostine on embryonic viability and development. *Cancer Res.* **66**, 8172-8181.

González-Rosa, J. M., Martín, V., Peralta, M., Torres, M. and Mercader, N. (2011). Extensive scar formation and regression during heart regeneration after cryoinjury in zebrafish. *Development* **138**, 1663-1674.

Grayfer, L. and Belosevic, M. (2009). Molecular characterization of tumor necrosis factor receptors 1 and 2 of the goldfish (Carassius aurutus L.). *Mol. Immunol.* **46**, 2190-2199.

Isogai, S., Horiguchi, M. and Weinstein, B. M. (2001). The vascular anatomy of the developing zebrafish: an atlas of embryonic and early larval development. *Dev. Biol.* **230**, 278-301.

Kimmel, C. B., Ballard, W. W., Kimmel, S. R., Ullmann, B. and Schilling, T. F. (1995). Stages of embryonic development of the zebrafish. *Dev. Dyn.* **203**, 253-310.

Krumschnabel, G., Sohm, B., Bock, F., Manzl, C. and Villunger, A. (2009). The enigma of caspase-2: the laymen's view. *Cell Death Differ.* **16**, 195-207.

Langheinrich, U., Hennen, E., Stott, G. and Vacun, G. (2002). Zebrafish as a model organism for the identification and characterization of drugs and genes affecting p53 signaling. *Curr. Biol.* **12**, 2023-2028.

Lawson, N. D. and Weinstein, B. M. (2002). In vivo imaging of embryonic vascular development using transgenic zebrafish. *Dev. Biol.* **248**, 307-318.

Locksley, R. M., Killeen, N. and Lenardo, M. J. (2001). The TNF and TNF receptor superfamilies: integrating mammalian biology. *Cell* **104**, 487-501.

Loetscher, H., Stueber, D., Banner, D., Mackay, F. and Lesslauer, W. (1993). Human tumor necrosis factor alpha (TNF alpha) mutants with exclusive specificity for the 55-kDa or 75-kDa TNF receptors. *J. Biol. Chem.* **268**, 26350-26357.

Luo, Y., Xu, Z., Wan, T., He, Y., Jones, D., Zhang, H. and Min, W. (2010). Endothelial-specific transgenesis of TNFR2 promotes adaptive arteriogenesis and angiogenesis. *Arterioscler. Thromb. Vasc. Biol.* **30**, 1307-1314.

MacEwan, D. J. (2002). TNF receptor subtype signalling: differences and cellular consequences. *Cell. Signal.* **14**, 477-492.

MacInnes, A. W., Amsterdam, A., Whittaker, C. A., Hopkins, N. and Lees, J. A. (2008). Loss of p53 synthesis in zebrafish tumors with ribosomal protein gene mutations. *Proc. Natl. Acad. Sci. USA* **105**, 10408-10413.

Mallo, M., Schrewe, H., Martin, J. F., Olson, E. N. and Ohnemus, S. (2000). Assembling a functional tympanic membrane: signals from the external acoustic meatus coordinate development of the malleal manubrium. *Development* **127**, 4127-4136.

Miura, A., Honma, R., Togashi, T., Yanagisawa, Y., Ito, E., Imai, J., Isogai, T., Goshima, N., Watanabe, S. and Nomura, N. (2006). Differential responses of normal human coronary artery endothelial cells against multiple cytokines comparatively assessed by gene expression profiles. *FEBS Lett.* **580**, 6871-6879.

Mosmann, T. (1983). Rapid colorimetric assay for cellular growth and survival: application to proliferation and cytotoxicity assays. *J. Immunol. Methods* **65**, 55-63.

Okada, Y., Kato, M., Minakami, H., Inoue, Y., Morikawa, A., Otsuki, K. and Kimura, H. (2001). Reduced expression of flice-inhibitory protein (FLIP) and NFkappaB is associated with death receptor-induced cell death in human aortic endothelial cells (HAECs). *Cytokine* **15**, 66-74.

Oliver, T. G., Meylan, E., Chang, G. P., Xue, W., Burke, J. R., Humpton, T. J., Hubbard, D., Bhutkar, A. and Jacks, T. (2011). Caspase-2-mediated cleavage of Mdm2 creates a p53-induced positive feedback loop. *Mol. Cell* **43**, 57-71.

Paik, E. J. and Zon, L. I. (2010). Hematopoietic development in the zebrafish. *Int. J. Dev. Biol.* **54**, 1127-1137.

Pfaffl, M. W. (2001). A new mathematical model for relative quantification in real-time RT-PCR. *Nucleic Acids Res.* **29**, 45e.

Roca, F. J., Mulero, I., López-Muñoz, A., Sepulcre, M. P., Renshaw, S. A., Meseguer, J. and Mulero, V. (2008). Evolution of the inflammatory response in vertebrates: fish TNF-alpha is a powerful activator of endothelial cells but hardly activates phagocytes. *J. Immunol.* **181**, 5071-5081.

Rothe, M., Pan, M. G., Henzel, W. J., Ayres, T. M. and Goeddel, D. V. (1995). The TNFR2-TRAF signaling complex contains two novel proteins related to baculoviral inhibitor of apoptosis proteins. *Cell* **83**, 1243-1252.

Ruemmele, F. M., Beaulieu, J. F., O'Connell, J., Bennett, M. W., Seidman, E. G. and Lentze, M. J. (2002). The susceptibility to Fas-induced apoptosis in normal enterocytes is regulated on the level of cIAP1 and 2. *Biochem. Biophys. Res. Commun.* **290**, 1308-1314.

Santoro, M. M., Samuel, T., Mitchell, T., Reed, J. C. and Stainier, D. Y. (2007). Birc2 (clap1) regulates endothelial cell integrity and blood vessel homeostasis. *Nat. Genet.* **39**, 1397-1402.

Schneider, K., Potter, K. G. and Ware, C. F. (2004). Lymphotoxin and LIGHT signaling pathways and target genes. *Immunol. Rev.* **202**, 49-66.

Schulte-Merker, S., van Eeden, F. J., Halpern, M. E., Kimmel, C. B. and Nüsslein-Volhard, C. (1994). no tail (ntl) is the zebrafish homologue of the mouse T (Brachyury) gene. *Development* **120**, 1009-1015.

Sepulcre, M. P., López-Muñoz, A., Angosto, D., García-Alcazar, A., Meseguer, J. and Mulero, V. (2011). TLR agonists extend the functional lifespan of professional phagocytic granulocytes in the bony fish gilthead seabream and direct precursor differentiation towards the production of granulocytes. *Mol. Immunol.* **48**, 846-859.

Sethi, G., Sung, B., Kunnumakkara, A. B. and Aggarwal, B. B. (2009). Targeting TNF for treatment of cancer and autoimmunity. *Adv. Exp. Med. Biol.* **647**, 37-51.

Shalaby, M. R., Sundan, A., Loetscher, H., Brockhaus, M., Lesslauer, W. and Espevik, T. (1990). Binding and regulation of cellular functions by monoclonal antibodies against human tumor necrosis factor receptors. *J. Exp. Med.* **172**, 1517-1520.

Shu, H. B., Takeuchi, M. and Goeddel, D. V. (1996). The tumor necrosis factor receptor 2 signal transducers TRAF2 and c-IAP1 are components of the tumor necrosis factor receptor 1 signaling complex. *Proc. Natl. Acad. Sci. USA* **93**, 13973-13978.

Sidi, S., Sanda, T., Kennedy, R. D., Hagen, A. T., Jette, C. A., Hoffmans, R., Pascual, J., Imamura, S., Kishi, S., Amatruda, J. F. et al. (2008). Chk1 suppresses a caspase-2 apoptotic response to DNA damage that bypasses p53, Bcl-2, and caspase-3. *Cell* **133**, 864-877.

Stanton, S. E., McReynolds, L. J., Evans, T. and Schreiber-Agus, N. (2006). Yaf2 inhibits caspase 8-mediated apoptosis and regulates cell survival during zebrafish embryogenesis. *J. Biol. Chem.* **281**, 28782-28793.

Taylor, R. C., Cullen, S. P. and Martin, S. J. (2008). Apoptosis: controlled demolition at the cellular level. *Nat. Rev. Mol. Cell Biol.* **9**, 231-241.

Traver, D., Paw, B. H., Poss, K. D., Penberthy, W. T., Lin, S. and Zon, L. I. (2003). Transplantation and *in vivo* imaging of multilineage engraftment in zebrafish bloodless mutants. *Nat. Immunol.* **4**, 1238-1246.

Westerfield, M. (2000). *The Zebrafish Book. A Guide for the Laboratory Use of Zebrafish Danio* (Brachydanio) rerio*. Eugene, OR: University of Oregon Press.

Wrasidlo, W., Mielgo, A., Torres, V. A., Barbero, S., Stoletov, K., Suyama, T. L., Klemke, R. L., Gerwick, W. H., Carson, D. A. and Stupack, D. G. (2008). The marine lipopeptide somocystinamide A triggers apoptosis via caspase 8. *Proc. Natl. Acad. Sci. USA* **105**, 2313-2318.